4D Computed Tomography Reconstruction from Few-Projection Data via Temporal Non-local Regularization

Xun Jia[1], Yifei Lou[2], Bin Dong[3], Zhen Tian[1,4], and Steve Jiang[1]

[1] Department of Radiation Oncology University of California, San Diego, La Jolla, CA 92037-0843, USA
[2] Department of Mathematics, University of California, Los Angeles, Los Angeles, CA 90095-1555, USA
[3] Department of Mathematics, University of California, San Diego, La Jolla, CA 92093-0112, USA
[4] Department of Biomedical Engineering, Graduate School at Tsinghua University, Shenzhen, Guangdong 518055, China

Abstract. 4D computed tomography (4D-CT) is an important modality in medical imaging due to its ability to resolve patient anatomy motion in each respiratory phase. Conventionally 4D-CT is accomplished by performing the reconstruction for each phase independently as in a CT reconstruction problem. We propose a new 4D-CT reconstruction algorithm that explicitly takes into account the temporal regularization in a non-local fashion. By imposing a regularization of a temporal non-local means (TNLM) form, 4D-CT images at all phases can be reconstructed simultaneously based on extremely under-sampled x-ray projections. Our algorithm is validated in one digital NCAT thorax phantom and two real patient cases. It is found that our TNLM algorithm is capable of reconstructing the 4D-CT images with great accuracy. The experiments also show that our approach outperforms standard 4D-CT reconstruction methods with spatial regularization of total variation or tight frames.

1 Introduction

Four-dimensional Computed Tomography (4D-CT) is one of the most important topics in medical imaging field that attract tremendous interests nowadays. In addition to providing three dimensional volumetric anatomical information as in conventional CT, 4D-CT is capable of resolving organ motions due to, for example, patient respiration by reconstructing a set of CT images corresponding to different respiratory phases in a breathing cycle. Such an imaging modality is particularly of use in many clinical applications regarding thorax or upper abdomen area, where a considerable amount of blurring artifacts would appear, if conventional CT is used instead.

In 4D-CT acquisition, x-ray projection data are usually extensively oversampled. Those projections are then grouped according to their associated respiratory phase information and 4D-CT are accomplished by reconstructing tomography images corresponding to different phases independently [1] as in a

conventional CT reconstruction problem. Since the current commercial standard Filtered Back Projection (FBP) algorithm [2] used to reconstruct each individual phase usually requires hundreds of projections to achieve decent quality, the 4D-CT reconstruction scheme demands an extremely large number of x-ray projections. The consequent long acquisition process therefore leads to an excess amount of radiation dose to the patient, potentially elevating cancer risks.

One obvious way of reducing the imaging dose in 4D-CT is to reconstruct the CT images of each breathing phase from fewer x-ray projections. However, the images reconstructed by conventional FBP-type algorithms would be severely degraded due to insufficient sampling. Recently, a bloom of vast and exciting research in compressed sensing [3, 4] has demonstrated the feasibility of recovering signals from incomplete measurements through optimization methods, providing us new perspectives of solving the CT reconstruction problem. Though this approach allows us to retrieve CT images in each phase with only a few number of projections, the total number of projections used for an entire 4D-CT reconstruction is still large due to many breathing phases to be considered. Therefore, it is highly desirable to develop new techniques to reconstruct 4D-CT with a greatly reduced number of projections, while image quality can still be well maintained.

One idea deeply buried in all approaches currently applied to the 4D-CT reconstruction is that images at different respiratory phases are reconstructed individually. Nevertheless, 4D-CT images in a breathing cycle are never independent of each other due to the smooth breathing pattern. Taking this temporal correlation into account can in principle facilitate the 4D-CT reconstruction process and potentially achieve the goal of even lowering projection number. In fact, it is reasonable to believe that there are usually common anatomical feathers within successive CT images, though the precise locations of those feathers may slightly vary. Inspired by this fact, we propose in this work a new 4D-CT reconstruction approach by imposing regularization among neighboring phases via a *Temporal Non-local Means* (TNLM) method. Specifically, each feature in a CT image is searched in nearby area in images of neighboring breathing phases and similar features are grouped together to constructively enhance each other. Such an approach is found to be capable of solving the few-view 4D-CT reconstruction problem, as will be seen in the rest of this paper.

2 Our Method

2.1 Conventional CT Reconstruction

Before presenting our method, we first describe how a conventional CT image is reconstructed from highly under-sampled projections. In fact, the conventional CT reconstruction problem, challenging by itself, is a subproblem of the 4D-CT reconstruction, if each phase is reconstructed independently. Let us denote one horizontal slide of patient anatomical information by a vector f. An x-ray projection matrix P maps f into another vector Y on x-ray detectors in a fan-beam geometry, such that $Pf = Y$. A CT reconstruction problem is formulated

as the retrieval of the vector f based on the observation Y given the projection matrix P.

The so-called few-projection CT reconstruction problem is well known to be highly under-determined in that there are infinitely many solution vectors f satisfying the equation $Pf = Y$. In order to single out an ideal CT image f, additional information needs to be imposed properly. For this purpose, regularization models are usually used to reconstruct a desirable CT image in this highly under-sampling situation. As such, one considers the optimization problem

$$f = \text{argmin}_f \|Pf - Y\|_2^2 + \frac{\mu}{2} J[f], \tag{2.1}$$

where the first term ensures the consistency between the reconstructed CT image f and the observation Y. The second term $J[f]$, known as a regularization term, is imposed a priori to guarantee that the reconstructed image from (2.1) satisfies some desirable properties, *e.g.* sharp in edges and smooth in homogeneous regions. Examples of $J[f]$ include *Total Variation* (TV) [5] and *Tight Frames* (TF) [6], to name a few. The parameter μ in (2.1) balances the fidelity of the solution f to the data Y and the imposed regularization.

It is straightforward to utilize this reconstruction approach to solve the 4D-CT reconstruction problem by applying it to each phase independently. The results produced by the TV-based or TF-based methods will be used to benchmark our 4D-CT reconstruction algorithm in our experiments.

2.2 4D-CT Reconstruction

Let us divide a respiratory cycle into N phases labeled by $\alpha = 1, \cdots, N$. Denote the CT image at phase α by a vector f_α. A projection matrix P_α at phase α maps the image into an observation vector Y_α, *i.e.* $P_\alpha f_\alpha = Y_\alpha$. As opposed to reconstructing images at each phase independently, we propose the following 4D-CT reconstruction model

$$\{f_\alpha\} = \text{argmin}_{\{f_\alpha\}} \sum_{\alpha=1}^{N} \|P_\alpha f_\alpha - Y_\alpha\|_2^2 + \frac{\mu}{2}[J(f_\alpha, f_{\alpha-1}) + J(f_\alpha, f_{\alpha+1})], \tag{2.2}$$

where $J(\cdot,\cdot)$ is a TNLM functional imposed as a temporal regularization term between successive phases. Specifically, for two images f_α and f_β, $J(f_\alpha, f_\beta)$ is defined as:

$$J(f_\alpha, f_\beta) = \iint [f_\alpha(x) - f_\beta(y)]^2 \, w_{f_\alpha^*, f_\beta^*}(x,y) \mathrm{d}x\mathrm{d}y. \tag{2.3}$$

The weighting factors $w_{f_\alpha^*, f_\beta^*}(x,y)$ are ideally independent of f_α, f_β but defined according to the ground truth images f_α^* and f_β^* as

$$w_{f_\alpha^*, f_\beta^*}(x,y) = \frac{1}{Z} \exp^{-\|p_{f_\alpha^*}(x) - p_{f_\beta^*}(y)\|_2^2 / h^2}, \tag{2.4}$$

where $p_{f^*_\alpha}(x)$ denotes a small patch in image f^*_α centering at the coordinate x and Z is a normalization factor. The scale parameter h controls to what extent similarity between patches is enforced.

The above definition of TNLM functional $J(\cdot,\cdot)$ resembles, and yet is fundamentally different from, the original *Non-local Means* (NLM) idea that have been widely used for restoring natural images [7, 8]. A key assumption in their approach is that a natural image, such as a photograph of buildings, usually contains some repetitive features. Therefore, the similarity between feathers at different locations can be utilized to constructively enhance each other for image restoration. In contrast, similar structures are hardly found in a single medical image. The efficacy of a direct application of the NLM to restore a single medical image, for example in CT reconstruction context, is thus limited. Nonetheless, the crucial similarity assumption naturally exists along a temporal direction, namely among images of adjacent phases. Therefore, in (2.2), we consider a TNLM regularization $J(f_\alpha, f_{\alpha\pm1})$ as opposed to $J(f_\alpha, f_\alpha)$ as in the NLM approach. Another reason why the TNLM is superior to the NLM method in this 4D-CT reconstruction problem is the capability of removing streaking artifacts (straight lines along CT projection directions), which usually present in highly under-sampled CT reconstruction problem (see the conventional FBP reconstruction results in Fig. 1). If NLM were used in the reconstruction, the streaking artifacts would be in fact strengthened rather than removed, since NLM method tends to locate those straight lines in a single image and enhance them. On the other hand, since the projection directions in two breathing phases are different, the streaking artifacts do not repeat in different phases. TNLM method is therefore able to remove them in all phases simultaneously.

To solve (2.2) efficiently, we adopt a forward-backward splitting algorithm [9, 10], where the solution to (2.2) can be obtained by alternatively performing the following two steps

$$v^k_\alpha = f^{k-1}_\alpha - \frac{1}{\lambda} P^T_\alpha (P_\alpha f^{k-1}_\alpha - Y_\alpha), \quad \forall\alpha, \tag{2.5}$$

$$\{f^k_\alpha\} = \mathrm{argmin}_{\{f_\alpha\}} \sum_\alpha \lambda \|f_\alpha - v^k_\alpha\|^2_2 + \frac{\mu}{2}[J(f_\alpha, f_{\alpha-1}) + J(f_\alpha, f_{\alpha+1})]. \tag{2.6}$$

Here v_α are auxiliary vectors and λ is a constant introduced by the splitting algorithm. Note that (2.5) is simply one step of gradient descent algorithm towards minimizing an energy functional $E[f_\alpha] = \sum_\alpha \|P_\alpha f_\alpha - Y_\alpha\|^2_2$ with a step size $1/2\lambda$. In order to speed up the convergence, we substitute this step by a conjugate gradient minimization for the energy functional $E[f_\alpha]$ with an initial solution f^{k-1}_α, denoted as $v^k_\alpha = \mathrm{CG}_{E[f_\alpha]}(f^{k-1}_\alpha)$. As for (2.6), we perform one step of gradient descent for each exterior iteration as

$$f^k_\alpha(x) = v^k_\alpha(x)(1-2\mu) + \mu \left[\int v^k_{\alpha+1}(y) w_{f^*_\alpha, f^*_{\alpha+1}}(x,y)\mathrm{d}y + \int v^k_{\alpha-1}(y) w_{f^*_\alpha, f^*_{\alpha-1}}(x,y)\mathrm{d}y \right]. \tag{2.7}$$

Note that, in the above equation, the images at phases $(\alpha \pm 1)$ are naturally imposed to enhance the image quality of f_α. Another issue worth mentioning here is the weighting factors $w_{f^*_\alpha, f^*_\beta}(x, y)$. In (2.4) they are defined with respect to the ground truth images f^*_α, which are not available during the reconstruction. In practice, for each iteration k, the weights $w_{f^*_\alpha, f^*_\beta}(x, y)$ are replaced by $w_{f^{k-1}_\alpha, f^{k-1}_\beta}(x, y)$. In summary, the algorithm solving (2.2) is to perform the following two steps alternatively:

$$\begin{aligned} v^k_\alpha &= \mathrm{CG}_{E[f_\alpha]}(f^{k-1}_\alpha), \quad \forall \alpha, \\ f^k_\alpha(x) &= v^k_\alpha(x)(1-2\mu) + \mu \left[\int v^k_{\alpha+1}(y) w_{f^{k-1}_\alpha, f^{k-1}_{\alpha+1}}(x, y) \mathrm{d}y \right. \\ &\qquad \left. + \int v_{\alpha-1}(y) w_{f^{k-1}_\alpha, f^{k-1}_{\alpha-1}}(x, y) \mathrm{d}y \right]. \end{aligned} \tag{2.8}$$

3 Experiments

We first test our 4D-CT reconstruction algorithm on a digital NCAT thorax phantom [11]. We consider a simple breathing model with only two phases in a respiratory cycle. The image resolution is 256×256. Due to its simple anatomical structure in this digital phantom, only 20 x-ray projections per respiratory phase are used. These projections are generated in a fan beam geometry and are equally spaced in an entire 360° rotation. In Fig. 1, we show the ground truth images and the reconstruction results from the conventional FBP algorithms in the first and the second columns, respectively. Clearly, FBP algorithm produces severe streaking artifacts in this context of extremely under-sampling, making these images clinically unacceptable. The reconstruction results shown in the columns 3 and 4 in Fig. 1 correspond to TV and TF methods. Despite a

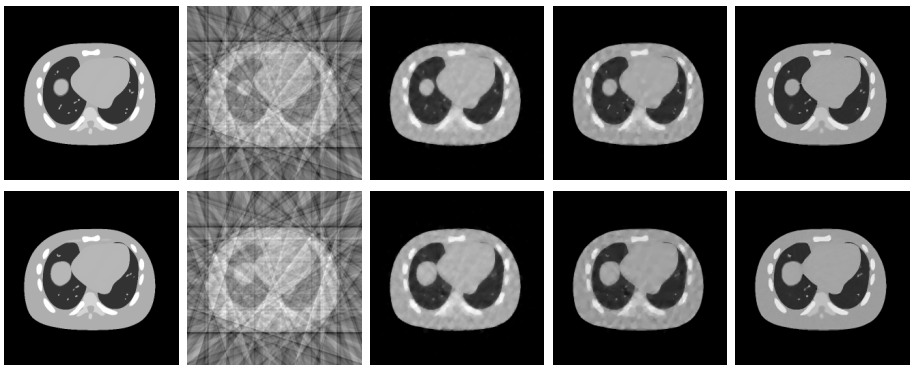

Fig. 1. A Digital NCAT phantom case. Images at two breathing phases are shown in two rows. Columns from left to right: ground truth images, reconstruction results from FBP, TV, TF, and our TNLM method, respectively.

great improvement over the FBP algorithm, the images obtained from these two methods are smeared out with reduced contrast and still contain obvious fluctuating artifacts. Finally, the images reconstructed from our TNLM regularization method are shown in the last column, where the image quality is considerably enhanced by imposing the temporal regularization between these two phases. Notice that for these iterative methods (TV, TF and TNLM), the results are presented with parameters, such as μ in Eq. (2.1), carefully tuned for the optimal results.

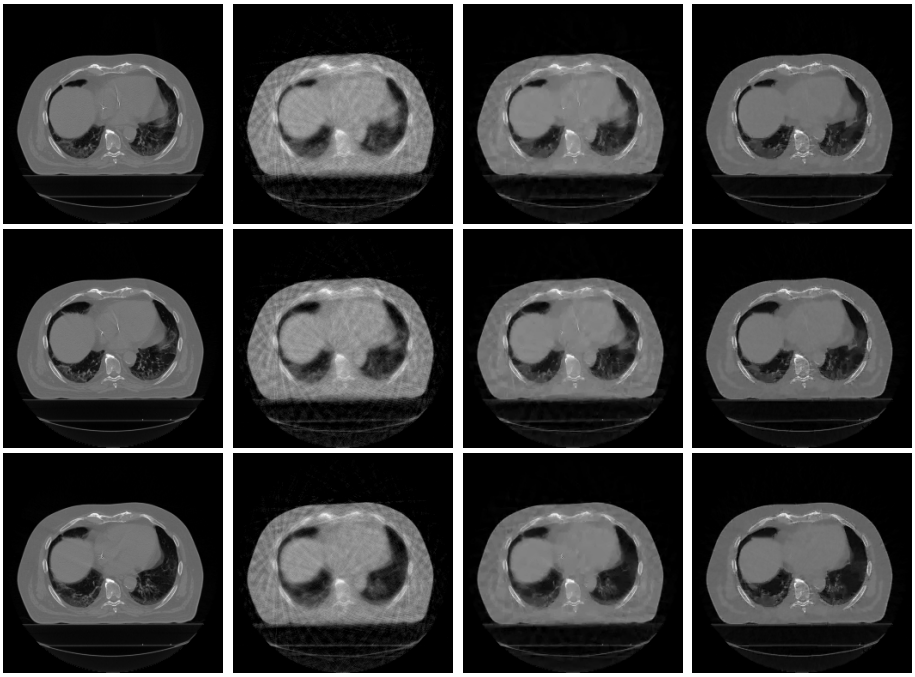

Fig. 2. Patient case A. Rows from top to bottom: phase 1, 4, and 7 in a 10-phase respiratory cycle. Columns from left to right: ground truth images, reconstruction results from TV, TF, and our TNLM method.

To further validate our 4D-CT reconstruction algorithm, we study two patient cases obtained in the real clinic. There are 10 breathing phases in both cases. Since the real clinical 4D-CT images are full of detailed structures, 30 fan beam x-ray projections per breathing phase are used. Other parameters are same as those in the NCAT phantom case. We exclude presenting the FBP results since it is apparently not able to provide clinically acceptable 4D-CT images. Due to the space limitation, only phase 1, 4, and 7 out of the 10 phases in an entire breathing cycle are illustrated in Fig. 2 and 3 respectively for the two

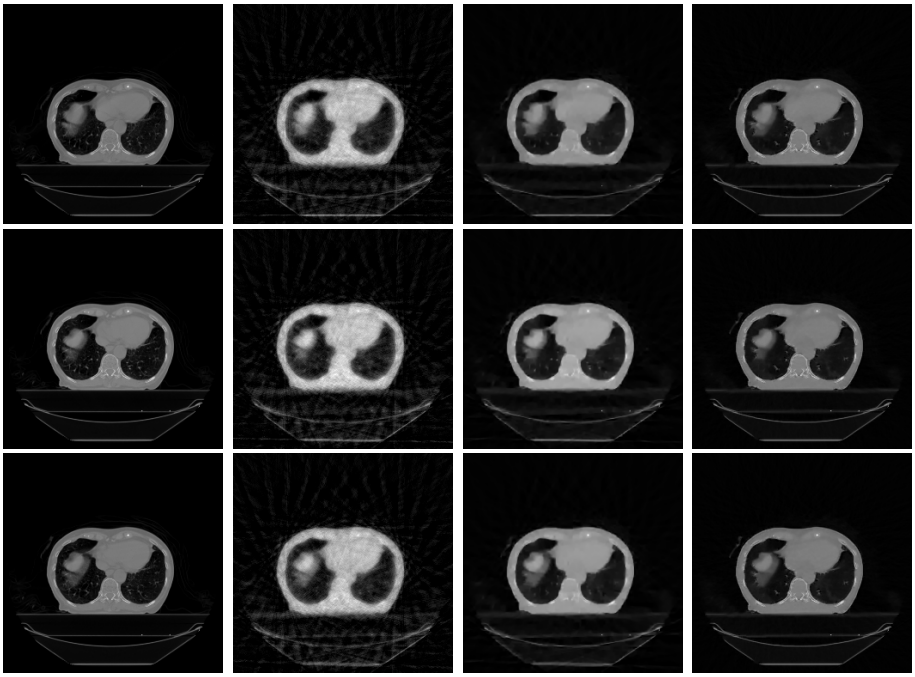

Fig. 3. Patient case B. Rows from top to bottom: phase 1, 4, and 7 in a 10-phase respiratory cycle. Columns from left to right: ground truth images, reconstruction results from TV, TF, and our TNLM method.

real clinical cases. Again, our method is able to reconstruct the 4D-CT images with great quality, while low contrast and streaking artifacts are found to some extent in those images obtained from TV or TF methods.

In order to quantitatively evaluate the reconstruction results, we take signal-to-noise ratio (SNR) as a metric defined as

$$\mathrm{SNR}(f^*, f) = 20 \log_{10} \left\{ \frac{||f - \bar{f}||_{L^2}}{||f - f^*||_{L^2}} \right\}, \tag{3.1}$$

where f^* is the ground truth image and $\bar{f}$ denote the mean value of the image f. The SNRs for images obtained from different methods are summarized in Tab. 1. Our method yield the highest SNR values in all cases, undoubtedly outperforms the other two methods.

4 Conclusion

In this paper, we have presented a new 4D-CT reconstruction algorithm that exploits the recurrence of the anatomical structures at different locations between

Table 1. SNR for different methods

	NCAT		patient A			patient B		
	Phase 1	Phase 2	Phase 1	Phase 4	Phase 7	Phase 1	Phase 4	Phase 7
TV	20.35	20.14	15.04	14.97	15.47	11.66	11.39	11.40
TF	21.06	20.72	18.71	18.66	19.46	15.85	15.44	15.14
our method	**25.68**	**25.59**	**20.63**	**20.29**	**20.44**	**18.99**	**19.22**	**19.13**

adjacent breathing phases. TNLM regularization is specifically designed to take this fact into the reconstruction process. We have tested our reconstruction results on one digital NCAT phantom and two patient cases. The reconstruction results indicate that our TNLM algorithm outperforms the conventional FBP-type reconstruction algorithm and the TV-based or TF-based spatial regularization methods. One concern about our TNLM method is the speed. Currently it takes much longer time for the TNLM method to reconstruct a set of 4D-CT images due to its inherent complicated mathematical structure. However, our preliminary work on the speed-up via advanced GPU technology indicates promising perspectives.

References

1. Low, D.A., Nystrom, M., Kalinin, E., *et. al.*: A method for the reconstruction of four-dimensional synchronized ct scans acquired during free breathing. Med. Phys. **30**(1254) (2003) 1254–1263
2. Deans, S.: The Radon Transform and Some of Its Applications. New York, Wiley (1983)
3. Candes, E.J., Romberg, J., Tao, T.: Robust uncertainty principles: exact signal reconstruction from highly incomplete frequency information. IEEE Transactions on Information Theory **52**(2) (2006) 489– 509
4. Donoho, D.L.: Compressed sensing. Ieee Transactions on Information Theory **52** (2006) 1289–1306
5. Rudin, L., Osher, S., Fatemi, E.: Nonlinear total variation based noise removal algorithms. Physics D **60** (1992) 259–268
6. Ingrid Daubechies, Bin Han, A.R.Z.S. Applied and Computational Harmonic Analysis (2003) 1–46
7. Buades, A., Coll, B., Morel, J.M.: A review of image denoising algorithms, with a new one. Multiscale Modeling and Simulation **4**(2) (2005) 490–530
8. Lou, Y., Zhang, X., Osher, S., Bertozzi, A.: Image recovery via nonlocal operators. Journal of Scientific Computing **42**(2) (2010) 185–197
9. Combettes, P., Wajs, V.: Signal recovery by proximal forward-backward splitting. Multiscale Modeling and Simulation **4**(4) (2006) 1168–1200
10. Hale, E., Yin, W., Zhang, Y.: A fixed-point continuation method for ℓ_1-regularization with application to compressed sensing. CAAM Technical Report TR, Rice University, Houston, TX (2007) 07–07
11. Segars, W.P.: Development and application of the new dynamic NURBS-based cardiac-torso (NCAT) phantom. PhD thesis, University of North Carolina, Chapel Hill (2001)